

Isochemical breakdown of garnet in orogenic garnet peridotite and its implication to reaction kinetics

Masaaki Obata¹, Kazuhito Ozawa², Kosuke Naemura² and Akira Miyake¹

¹ *Kyoto University, Department of Geology and Mineralogy, obata@kueps.kyoto-u.ac.jp*

² *University of Tokyo, Department of Earth and Planetary Sciences*

ABSTRACT

An isochemical kelyphite (orthopyroxene+spinel+plagioclase) that has nearly the same bulk chemical composition as the precursor garnet was found within a matrix of ordinary kelyphites (orthopyroxene+clinopyroxene+spinel±amphibole) in garnet peridotites from the Czech part of the Moldanubian Zone. It was shown that the kelyphitization of garnet took place in three stages: (1) the garnet-olivine reaction, accompanied by a long-range material transfer across the reaction zone, and (2) the isochemical breakdown of garnet, essentially in a chemically-closed system, and finally, (3) an open-system hydration reaction producing a thin hydrous zone (amphibole+spinel+plagioclase), which is located between the isochemical kelyphite and relict garnet. The presence of relict garnet suggests that this breakdown reaction of the second stage did not proceed to a completion probably being hindered by the formation of the hydrous zone at the reaction front. It was found by electron back-scattered diffraction method that orthopyroxene and spinel do not show any topotaxial relationship in the first type of kelyphite; whereas they show locally topotaxial relationship in the isochemical kelyphite. The transition from the first type to the second type of kelyphite is discussed on the basis of the detailed observations in the transition zone between the two kelyphites. More widespread occurrence of isochemical kelyphite is expected to occur in orogenic peridotites as well as from xenoliths brought by volcanics.

26

27 **INTRODUCTION**

28 It has been widely observed that pyrope garnet is partly or completely decomposed
29 into fine-grained symplectitic mineral intergrowths called ‘kelyphite’ when deep-sheeted
30 rocks are decompressed either by a tectonic emplacement of rock masses accompanied by
31 exhumation or by a more rapid transport of rock fragments to the Earth’s surface by
32 volcanic eruptions (i. e., xenoliths). Many kelyphites are rarely isochemical with the
33 precursor garnets and have been typically and significantly modified from their original
34 garnet compositions, implying that kelyphite is not a simple breakdown product of garnet
35 but a reaction product between garnet and its surroundings such as olivine (e.g., Obata
36 2011). ‘Isochemical kelyphite’ on the other hand have been reported to occur mostly from
37 xenolithic garnet pyroxenites or mafic granulites, such as those in nephelinitic breccia,
38 Delegate, Australia (Keankeo et al, 2000), in basanitic breccia, Sicily (Sapienza et al, 2001)
39 and those in alkali basalt and basaltic tuffs, Central Pannonian Basin, Hungary (Degi et al,
40 2010). We report in this paper a first clear occurrence of isochemical kelyphite, surrounded
41 by an ordinary non-isochemical kelyphite from orogenic garnet peridotites that occur in the
42 Czech part of the Moldanubian Zone. We demonstrate that the isochemical breakdown of
43 garnet took place after the formation of a non-isochemical kelyphite. The detailed study of
44 the kelyphitization processes, together with the analysis of their physical conditions of
45 formation will put important constraints on the exhumation history of the host peridotites
46 and the reaction kinetics.

47 **GEOLOGICAL BACKGROUND**

48 The Moldanubian Zone is a southern part of the European Variscan orogen which was
49 active at around 340 Ma. Its metamorphic core complex is well exposed in the Bohemian
50 Massif (Fig. 1). The Moldanubian Zone in the Bohemian Massif consists of three

51 metamorphic units: the Monotonous Unit, the Varied Unit and the Gföhl Unit, in the
52 structurally ascending order, where metamorphic grade increases in this order. The main
53 rock types of the Gföhl Unit are garnet-kyanite-bearing orthogneiss of peraluminous
54 granitic composition, subordinate amounts of pyroxene-bearing mafic granulite, garnet
55 amphibolite, and calc-silicate rocks. Numerous small masses of garnet peridotite occur
56 sporadically both in the granulite and migmatitic gneisses at many localities of the Gföhl
57 Unit and they have been classified into three types by Medaris et al (2005): Type I,
58 transformed from high-temperature spinel peridotite to garnet peridotite, which is
59 considered to be derived from "asthenospheric" mantle; Type II with Fe-Ti- rich
60 compositions and therefore considered to represent disrupted fragments of a mafic-
61 ultramafic cumulate complex; and Type III, equilibrated in a medium P/T regime and
62 considered to represent fragments of a deep mantle wedge.

63 The studied sample is a garnet-spinel-peridotite taken from a boudinage mass (5m
64 × 10m in size) of peridotite enclosed in a well-foliated felsic granulite in the Plešovice
65 quarry, which is located at the eastern edge of the Blansky les granulite massif (of the Gföhl
66 Unit)(Fig. 1). It is considered to belong to Type I of Medaris on the basis of a ubiquitous
67 presence of spinel inclusions in garnet (Naemura et al, 2009). It was shown that the garnet
68 peridotite was once equilibrated at 2.3–3.5 GPa and 850–1030°C in the upper mantle and
69 was then exhumed to the lower crustal level and got partially re-equilibrated in the spinel-
70 lherzolites facies (Naemura et al., 2009). The host granulite records a peak metamorphism
71 at around 750-850°C and 1.6-1.8 GPa (Stipska & Powell, 2005).

72 **OBSERVATIONAL METHODS AND ANALYTICAL TECHNIQUES**

73 Microstructural observation of kelyphites was made using a field-emission electron gun
74 scanning microscope (FE-SEM; JEOL 7000F) at the University of Tokyo. X-ray
75 compositional mapping and electron microprobe analysis were made using a wave-length

76 dispersive electron microprobe (WDS) both at the Univ. Tokyo and Kyoto University.
77 Quantitative analyses of minerals were made at Kyoto Univ. using WDS microprobe
78 (EPMA). Acceleration voltage of 15KV and beam current of 20 nA were used throughout.
79 For mineral analysis a focused electron beam (of ca. 3 μm size) was used and for bulk
80 analysis of kelyphites, a defocused electron beam (5 to 10 μm size) was used and many
81 analyses (typically 20 spot analyses) were averaged. A combination of both synthetic and
82 natural minerals was used as standards and ZAF correction was utilized. Crystallographic
83 orientation of minerals in the kelyphites was determined using an electron backscattered
84 diffraction system (EBSD) attached to the FE-SEM (HKL Nordlys detector with Channel
85 5) at the Univ. Tokyo. The transmission electron microscopic work (TEM) was made both
86 at Kyoto University and Kobe University. The thin foil preparation for the TEM
87 observation was made using a focused ion beam (FIB: FEI Quanta 200 3DS) at Kyoto
88 University and was observed with TEMs: H-8000k (Hitachi) at Kyoto University and
89 JEM2010 (JEOL co.) with NORAN System SIX (Thermo Fisher Scientific Inc.) at Kobe
90 University.

91 **PETROGRAPHIC DETAILS OF KELYPHITES**

92 The studied sample is a garnet-spinel peridotite of harzburgitic composition that is
93 comprised of olivine, orthopyroxene (Opx), clinopyroxene (Cpx), and garnet (Grt) and
94 spinel (Sp). Garnet typically forms large grains and is always, partially or completely,
95 kelyphitized. Olivine is moderately serpentinized but the kelyphite is, for most part, free
96 from secondary alteration except along rare fractures and/or veins. The majority part of the
97 kelyphite is a fine-grained, radial and fibrous intergrowth that consists of Opx, Cpx, and
98 spinel with subordinate amounts of Ca-amphibole (Amp). This type of kelyphite is referred
99 to as 'kelyphite I' hereafter (Fig. 2a). As is typical of this type, the microstructure of
100 kelyphite I is characterized by the occurrence of small elongated patches of Cpx enclosed in

101 much larger crystals of Opx, both of which include many regularly-spaced thin vermicular
102 lamellae of spinel defining a local lineament (Obata, 2011; Fig. 4a, b, d). Spinel lamella are
103 scarce or absent in amphibole crystals in kelyphite I. It is noted that the scale of kelyphite I
104 (i.e., the size of Cpx patches and the spacing of the spinel lamella) rapidly decreases, to that
105 of kelyphite II, in the vicinity of garnet and kelyphite II (Fig. 4b). In a more macroscopic
106 scale, kelyphite I is surrounded or enveloped by a narrow rim or ‘moat’ (0.2 – 0.5 mm
107 wide) that consists of polycrystalline coarse-grained Opx (grain size ca. 0.2 mm;
108 abbreviated as ‘COR’, standing for ‘Coarse Opx Rim’) separating the fine-grained kelyphite
109 inside from the olivine-dominant matrix outside, which is also typical of this type of
110 kelyphite (Fig. 2a; Obata & Ozawa, 2011; Obata, 2011).

111 Within a mass of kelyphite I, there occasionally occurs a region of much finer-
112 grained and darker-colored (in transmitted light) than kelyphite I (Fig. 2a, b). It was found
113 by X-ray mapping with an electron microprobe analyzer that this finer-grained part has
114 nearly the same bulk composition as the adjacent garnet (Fig. 3); and this new, extremely
115 fine-grained, isochemical kelyphite is referred to as ‘kelyphite II’. The kelyphite II part has
116 relatively low birefringence (under cross-polarized light) and has typically a domain
117 structure as recognized by the slight differences in interference colors and different
118 extinction angles in cross-polarized light (Fig. 2b) and distinct lineament structures as
119 described below. The boundary between kelyphite I and II is not necessarily sharp and a
120 narrow transition zone may be defined according to the texture and mineralogy, which will
121 be described in more details below. Very rarely relict garnets occur in association with
122 kelyphite II as well as kelyphite I. A peculiar textural feature of kelyphite II is that it is
123 developed only on one side of garnet (Fig. 2a), so that, unlike kelyphite I, kelyphite II does
124 not form a corona structure surrounding the garnet. Examination of many thin sections
125 from this locality revealed that such asymmetric (i.e., non-concentric) configuration is

126 universal wherever kelyphite II and relict garnet occur together and we refer to such
127 textural feature as the 'asymmetric nature' of kelyphite II.

128 The kelyphite II has a different mineral assemblage than the kelyphite I, which is
129 Opx+Sp+plagioclase (Pl) (An₉₉). (It is so fine-grained that phase identification was made
130 with the aid of combinations of EBSD and EDS attached to a FE-SEM.) Although kelyphite
131 II is mostly anhydrous, small amounts of amphibole occur in addition to Opx, Sp and
132 plagioclase at some margins of kelyphite II. Each domain of kelyphite II is characterized by
133 a very straight lineament, which is more straight than those in kelyphite I (Figs. 2b, 4b).
134 The lineament consists of fine intergrowths of laths of Opx and plagioclase, where spinel
135 occurs as discontinuous thin lamellae (less than 1 μm thick) exclusively within the Opx
136 laths (Fig. 4c). The Opx-Pl spacing is only a few microns, and accurate microprobe analysis
137 of these phases was not possible in kelyphite II. Sporadically, however, there are spots of
138 large granular grains of spinel and Opx, where microprobe analysis was possible (Fig. 4c).

139 A transition zone of up to 100 μm width may be defined between the kelyphite I and
140 kelyphite II (Fig. 4a) and this zone may be further subdivided into two subzones, according
141 to their characteristic mineral assemblages, B and C (Fig. 4d). The outer zone of the
142 transition zone, B, consists of Opx, Sp and amphibole and is composed of two structural
143 components in alternation: (a) fine symplectitic intergrowth of Opx and Sp, and (b) coarser
144 spinel-lamella-sparse amphibole (pargasite; of a few micron width, Fig. 4d). Texturally, the
145 Opx-spinel intergrowths appear to be continuous from those in the adjacent kelyphite I
146 (Zone A) to Zone B and even to Zone C (Fig. 4d). Moving from kelyphite I toward
147 kelyphite II, the extinction of Cpx defines the beginning of transition zone B. The
148 appearance of plagioclase defines the beginning of subzone C in the transition zone, where
149 Opx, spinel, plagioclase and amphibole coexist. The microstructure in this zone is more
150 erratic without any clear lineament in contrast to the adjacent kelyphite II (Zone D).

151 Plagioclase, a characteristic phase in Zone C, forms discrete round ‘pools’ of up to 10 μm
152 size, and thus microprobe analyses of plagioclase, and amphibole too, were barely possible
153 in this zone. The transition to kelyphite II is defined by the emergence of a clear lineament
154 of the symplectitic structure and the grain size reduction. A small amount of amphibole
155 remains in the margins (up to tens of microns width) of kelyphite II. The proportion of
156 Zone B to C varies greatly in the transition zone. On a left-side boundary (Fig. 4d) Zone B
157 is thinner than Zone C and is even locally missing, where kelyphite I is in direct contact
158 with Zone C; whereas at a right-side corner adjacent to garnet (Fig. 4e), Zone B is widely
159 developed and is in direct contact with kelyphite II or relict garnet without Zone C, where
160 the lineament in Zone B is sharply truncated by that of kelyphite II. It is noted that Zone B,
161 although narrow, partly envelopes the garnet, where kelyphite II is not developed (Fig. 4a,
162 e), implying that Zone B may be regarded as a genetic extension of kelyphite I. It is also
163 noted that the lamella spacing of Zone-B kelyphite becomes rapidly reduced, as in kelyphite
164 I, approaching the garnet (Fig. 4e).

165 Facing to the garnet, kelyphite II is separated from the relict garnet by a narrow
166 zone of another kind of symplectite (10 to 20 μm width) that consists of amphibole, spinel
167 and subordinate amounts of plagioclase; this boundary zone will be referred to as ‘kelyphite
168 III’ in this paper (Figs. 1, 4a, 4b, 4e). (The phase identification in kelyphite III was
169 confirmed with TEM in addition to the EBSD and EDS analyses.) Although there occurs
170 locally a slight kink in direction in the spinel lamellae across the kelyphite II and III
171 boundary (Fig. 4e), the lineament is on average nearly normal to the garnet grain boundary
172 as the kelyphite I against garnet. Chemically, kelyphite III is not isochemical to garnet and
173 contains more Ca and Na (and therefore, less Mg and Fe) than the garnet (and thus
174 kelyphite II) as described below (Fig. 3; Table 1).

175

176 **CRYSTALLOGRAPHIC ORIENTATION RELATIONSHIPS**

177 The EBSD analysis of the kelyphites revealed that the kelyphite I has the same
178 features as observed for the lower-temperature group of kelyphite as described in Obata and
179 Ozawa (2011). That is, kelyphite I consists of multiple domains of single crystal of Opx
180 and, within each Opx domain, Cpx patches have all the same crystallographic orientation
181 and show a common systematic crystallographic relationship with their host Opx by sharing
182 their (100] and (010) and [001]. Amphibole, wherever it occurs, also show the same
183 crystallographic relationship with Cpx and Opx by sharing their (100) and (010) and [001].
184 (Such systematic crystallographic relationship is referred to as ‘topotaxy’ according to the
185 suggestion of IMA: Bailey et al., 1977). Spinel, on the other hand, does not show any
186 systematic relationship with Opx or Cpx, just similar to the garnet peridotite from
187 Norwegian Caledonide, whose kelyphitization temperature was estimated to be 700~760 °C
188 (Obata and Ozawa, 2011)

189 The topotaxic relationship is, however, more complicated and variable in kelyphite
190 II in the same sample. It was revealed that, within each domain of kelyphite II,
191 crystallographic axes of the Opx is nearly constant in direction (except the coarse granular
192 Opx grains, Fig. 4c) with some scatter, up to 15° in the Euler angle, which indicates that the
193 Opx crystal laths are probably all crystallographically connected to each other in the three
194 dimensions within the same domain forming a large (and spongy) single crystal of Opx. It
195 is revealed, therefore, that the interference color observed optically (Fig. 2b) represents
196 essentially that of Opx. It is also noted that the elongation of each Opx crystal lath or
197 lamella is not related to any simple crystallographic direction or crystallographic axis of
198 Opx. This morphological independency from crystallographic axes is more evident where
199 curvature occurs in the Opx laths assembly within the same domain, where crystallographic
200 orientation of Opx (as examined by EBSD) is remarkably constant regardless of the

201 curvature, indicating that the curvature is primary in origin and not due to secondary
202 deformation. Across domain boundaries, however, the lineament changes abruptly and
203 discontinuously and so does the crystallographic orientation of the Opx, thereby defining
204 the domain boundary (Fig. 4b).

205 The crystallographic orientation of the spinel is more erratic and variable even
206 within the same domain of kelyphite II and so is the crystallographic relationship between
207 the spinel and the host Opx. There is a clear tendency that, well inside an Opx domain
208 (such as around point (c) in Fig. 2b), spinel tends to have the same topotaxial relationship
209 with the Opx as is observed in the 'higher-temperature' kelyphites (i.e., Czech Mohelno
210 peridotite: Obata and Ozawa, 2011) or pyroxene-spinel symplectites from the Horoman
211 peridotite (Odashima et al., 2008); that is, one of four equivalent $\{111\}$ of spinel coincides
212 with pyroxene (100) and one of six equivalent $\{110\}$ of spinel coincides with pyroxene
213 (010) (Fig. 5 (c)). Near the outer margin of kelyphite II and also close to the garnet (i.e.,
214 kelyphite III) within the same domain of Opx, however, such topotaxial relationship is
215 broken and spinel shows more scattered and more random pattern of orientations (Fig. 2b,
216 points (b) and (d); Fig 5 (b), (d)). Such changes of crystallographic relationship seem to be
217 gradational from one to the other within the same domain although the crystallographic
218 orientation of the host Opx is constant (Fig. 5(a)).

219 In kelyphite III, the amphiboles have nearly the same crystallographic orientation
220 with the adjacent Opx, shearing their [100] and [010] directions and the [001] axis
221 (compare Fig. 6(a) with Fig. 5(a)); whereas, spinel shows a random pattern as is observed
222 in the immediate adjacency in kelyphite II (Fig. 6(b)).

223 **MINERAL AND BULK CHEMICAL COMPOSITIONS OF KELYPHITES**

224 Bulk compositions of the three kinds of kelyphites, I, II, and III, were obtained with
225 EPMA using a defocused electron beam and the results are listed and compared with the

226 garnet composition in Table 1; other microprobe analyses of minerals are listed in Table 2.
227 It was confirmed that kelyphite II is nearly isochemical, at least in term of major elements,
228 with the adjacent (i. e., precursor) garnet. In more details, however, kelyphite II contains
229 slightly more Na (0.04 Na₂O wt%) than the garnet. Amphibole bearing margins and the
230 vicinity of the fracture veins cutting across the kelyphite ('f' in Fig. 4a), where slight
231 depletion of Ca and enrichment of Na are recognized (Fig. 3), were avoided in the bulk
232 analyses of kelyphite II. The garnet is homogenous except near the grain edges facing to
233 kelyphite I (within a few tens of microns from the boundary), where a significant rim-ward
234 increase in the Fe-Mg ratio is noted (Table 2). Such zoning does not occur at the edges
235 facing to kelyphite II (or, more precisely, kelyphite III). Kelyphite I, on the other hand, is
236 significantly higher in MgO and lower in Al₂O₃ in bulk contents than the garnet, which is
237 typical for this type of kelyphite (Obata, 2011). Kelyphite III is distinct from kelyphite II in
238 that it has higher CaO and Na₂O contents (Table 2). It is noted that transition subzones,
239 both B and C, are not isochemical to garnet but their heterogeneities hindered us to obtain
240 good average compositions even using a defocused electron beam. Plagioclase in Zone C is
241 very calcic; its anorthite content being 99 mole %. Although accurate analysis was not
242 possible for the plagioclase in kelyphite II, semi-quantitative analysis using EDS attached
243 to FE-SEM revealed that the plagioclase in kelyphite II is highly calcic as in Zone C. The
244 amphibole in transition subzone B and kelyphite III is variable but all quite aluminous (13.3
245 to 17.5 in Al₂O₃ wt %) and sodic, being pargasitic (Table 2). The Al₂O₃ content of Opx is
246 3.7 wt% in kelyphite I and that of kelyphite II (the large grains) is 4.0 wt%. The
247 composition of spinel in kelyphite III is inferred by semi-quantitative analysis using EDS
248 attached to TEM to be: Cr# (Cr/(Cr+Al) in mole) = 0.05~0.16 and Mg# (Mg/(Mg+Fe) in
249 mole) = 0.61-0.73, which covers the compositional range of that in kelyphite II (Table 2).
250 The plagioclase in kelyphite III is more sodic than those in kelyphite II, being in the range

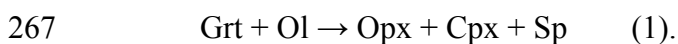
251 of An₈₀₋₉₀. The bulk analysis obtained for the Opx-spinel symplectite in Zone B (marked 's'
252 with a white circle in Fig. 4e) using a defocused electron beam (of 5 µm diameter) (No. 11,
253 Table 2) may satisfactorily be modeled in terms of a mechanical mixture of Opx and spinel,
254 of 3:7 in weight (equivalent to 1:2 in volume), using the microprobe analyses of respective
255 phases in kelyphite II (i.e., Nos. 4 and 6, Table 2).

256 **DISCUSSION**

257 **A sequence of kelyphitization processes**

258 It is inferred from textural relationships that kelyphite I first formed and then
259 kelyphite II, and finally terminated with the formation of kelyphite III. The question to be
260 raised here is how these events are related in physical conditions and in time, and what the
261 critical factors that controlled the kelyphitization processes were. The key to understand the
262 mode of transition in the formation of kelyphite I to kelyphite II may be contained in the
263 transition zone.

264 It is conceivable that kelyphite I was formed, when garnet peridotite was subjected
265 to a decompression and brought into the spinel-lherzolite stability field, by a well-studied
266 reaction between garnet and olivine (e.g., Kushiro and Yoder, 1966) :



268 The temperature at which this reaction took place has been estimated to be 730–770°C by
269 employing the two-pyroxene geothermometer of Taylor (1998) to the microprobe analyses
270 of pyroxenes in kelyphite I (Naemura et al, 2009). Note that garnet itself can still be stable
271 as a single phase although the garnet became thermodynamically incompatible with olivine
272 at this stage. The inner, fine-grained symplectite (i.e., kelyphite I) is interpreted to be after
273 garnet, whereas the outer, coarse Opx rim (COR) be after olivine (Obata and Ozawa, 2011;
274 Obata, 2011). These replacement reactions for garnet and olivine, respectively, are both
275 open-system reactions and there must have been significant long-range material transfer

276 across the reaction zone between the two reaction fronts (Obata, 2011). The presence of the
277 remnant garnet (i.e., kelyphite II in this case) implies that reaction (1) did not proceed to
278 completion but ceased at some point. It is conceivable that the reaction had slowed down as
279 the reaction zone widened probably because of the decrease of the chemical potential
280 gradients in the reaction zone. A progressive increase of the internal stress due to the
281 volume-increase nature of the reaction (Obata, 2011) may also be a factor in decelerating
282 the process (Milke et al, 2009; Schmid et al, 2009), and thereby punctuating the formation
283 stage of kelyphite I.

284 Upon further ascent and decompression in the rocks, garnet itself will eventually
285 become unstable, and beyond some critical level of decompression, the remaining garnet
286 will start to break down by itself as follows:



288 The proportion of the product phases, Opx, Sp, and Pl, in the studied kelyphite is calculated
289 to be 52:16: 32 (in wt%), from a mass balance calculation using mineral microprobe
290 analyses and the bulk composition of the kelyphite (Table 2). A relevant reaction that may
291 define the lower stability limit of garnet in mafic systems would be:



293 whose equilibrium position has been experimentally determined in the CaO-MgO-Al₂O₃-
294 SiO₂ system (Kushiro and Yoder, 1966; Gasparik, 1984; Fig. 7). In their model, the garnet
295 composition was assumed to be Py₂Gr₁ (i.e., Ca/(Ca+Mg)=0.333 in mole). The garnet
296 studied here is less calcic than this and its Ca/(Ca+Mg+Fe) value is 0.17 (in mole), which
297 may account for the absence of Cpx in the assemblage of the studied kelyphite II.

298 Theoretically, such less-calcic garnet can become unstable at higher pressures than that of
299 the equilibrium position of reaction (3). It should be noted here that reaction (2) must have
300 taken place irreversibly far from equilibrium because it does not appear to have been

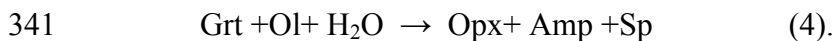
301 accompanied by a diffusion-aided compositional adjustment of garnet (to an equilibrium
302 composition). The pressure at which the irreversible reaction (2) actually took place,
303 therefore, is indeterminable; it could be higher (but below the pressure of reaction
304 (1))(Point 2 in Fig. 7) or lower than the equilibrium pressure of reaction (3)(Point 2' in Fig.
305 7). If the former were the case, i.e., kelyphite II formed at relatively higher pressure (Point
306 2 in Fig. 7), the formation of kelyphite II may not have been significantly separated in time
307 from the kelyphite I formation and the kelyphitization processes, from I to II, may have
308 been a single continuous event. If the latter were the case, there must have been a
309 considerable time interval between the two events of kelyphitization in order for a
310 considerable cooling (and decompression) is allowed to occur (from Point 1 to Point 2', Fig.
311 7). In either case it is important to note that the isochemical breakdown of garnet started to
312 occur at some points on the grain boundaries, not inside the crystal, and the kelyphite grew
313 inward replacing the garnet, forming a sharp and migrating reaction front.

314 A question then arises as to why reaction (2) did not proceed to a completion,
315 thereby eliminating all the garnet. The argument of volume-increase and stress building-up
316 as made for kelyphite I above may also be applicable here. Unlike reaction (1), reaction (2)
317 does not require a long-range material transfer and may be regarded as a kind of
318 polymorphic transition in the sense that long-range element diffusion is not required. The
319 situation may be analogous to the occurrence of metastable coesite surrounded by
320 polycrystalline quartz (the 'palisade quartz') that occurs within a garnet crystal (Chopin,
321 1984). The reaction is said to have ceased because of the elevation of internal stress brought
322 about by the progress of the volume-increase, coesite-to-quartz transformation reaction in a
323 restricted volume within the garnet host (Gillet et al, 1984). Unlike the 'palisade' quartz,
324 however, kelyphite II is typically developed only at one side of garnet – the asymmetry.
325 (The origin of the asymmetry is discussed below.) Moreover, the relict garnet is sheltered

326 from kelyphite II by another thin film of hydrous symplectite – kelyphite III. Such
327 occurrence implies that the formation of kelyphite III may have played some role for the
328 cessation of reaction (2). As opposed to reaction (2), however, the formation of kelyphite
329 III, although the reaction has not been identified yet, must have been accompanied by a
330 significant long-range material transfer, as well as the introduction of water. The fracture
331 veins running through the kelyphite II region (Figs. 4a) might represent relicts of such a
332 fluid pathway. The observed geochemical anomalies around the vein may be the result of
333 fluid-rock interaction. Admittedly it sounds paradoxical that an introduction of fluid leads
334 to a cessation of the breakdown reaction of garnet. More detailed processes and exact
335 mechanisms of such a hypothetical hydration reaction are the subject for future research.

336 **Origin of the transition zone**

337 Considering the microstructural continuity, subzone B of the transition zone is thought to
338 represent a very late stage of kelyphite I. It is conceivable that, as temperature decreases
339 during the advance of kelyphitization, amphibole replaces clinopyroxene if the activity of
340 H₂O is sufficiently high, where reaction (1) switches to another, hydration reaction as,



342 This inference is consistent with the local and incipient development of Zone B partially
343 enveloping the garnet crystal where kelyphite II is not developed (Figs. 4a, 4e). On the
344 other hand, subzone C may represent the onset of reaction (2), where a nucleation of a new
345 phase plagioclase had occurred. Opx, spinel and amphibole, on the other hand, did not
346 have to nucleate and probably simply continued to grow from subzone B on the expense of
347 garnet, thereby maintaining the microstructural continuity as observed. At very early stages
348 of reaction (2), the system may not have been completely closed and there may have been
349 some chemical interactions via material transfer with the surroundings probably with the
350 aid of intergranular fluids. The presence of amphibole and the coarser-grained nature of

351 subzone C implies the presence of some intergranular aqueous fluids at this stage, which
352 may have promoted some long-range material transfer and grain coarsening and thus
353 causing a local deviation from the original garnet composition. As subzone C grows
354 replacing garnet, the limited amount of water will be consumed by the formation of
355 amphiboles and the system will become desiccated and closed chemically, grading rapidly
356 into the anhydrous, isochemical kelyphite – kelyphite II.

357 Another possibility to be considered is that of the secondary origin for the transition
358 zone. The transition zone, particularly subzone C, might represent a secondary alteration
359 zone that was developed around a primary interface between the kelyphite I and kelyphite II
360 zones. Such a locally-selective secondary recrystallization could have occurred if some
361 aqueous fluid was introduced along the primary zone boundary. Lack of lateral continuity
362 of subzone B may be ascribed to such a secondary modification but the microstructural
363 continuity observed *across* the transition zone is not favorable to this hypothesis.

364 **Considerations on reaction kinetics and the origin of topotaxy**

365 A comparison with other occurrences of isochemical kelyphite reported in literature
366 would give some insights to reaction kinetics for the garnet breakdown. The isochemical
367 kelyphite from the Delegate garnet pyroxenite xenoliths consists of *clinoferrosilite*,
368 anorthite and spinel (Keankeo et al, 2000). The clinoferrosilite is said to be after
369 protoenstatite, which implies considerably high temperatures for the isochemical
370 breakdown of garnet, being definitely above 1000°C. The fine-grained nature of the
371 Delegate samples was ascribed to a rapid growth of kelyphite probably resulting from a
372 rapid ascent and rapid decompression of the xenolith brought up by volcanics (Keankeo et
373 al, 2000). The fine-grained nature of the studied Czech sample, however, cannot be
374 ascribed to a rapid ascent like the xenoliths but rather has to be ascribed to a rapid growth,
375 which is not necessarily related with the ascent rate. It should be noted that the first

376 kelyphitization (kelyphite I) took place at considerably lower temperatures ($< 800^{\circ}\text{C}$) for
377 the Czech sample than the Delegate xenoliths. The temperature of the second
378 kelyphitization (kelyphite II) cannot be determined precisely because of the lack of an
379 appropriate geothermometer for this mineral assemblage, but it is likely to be below that of
380 kelyphite I considering the inferred P - T history and the geotectonic setting (Naemura et al,
381 2009; Fig. 7). The inferred rapid growth of kelyphite II, therefore, must be ascribed to a
382 high degree of super-saturation (i.e., far from equilibrium) and a strong irreversibility of the
383 reaction, which may become possible at relatively low temperatures as discussed for
384 kelyphite I by Obata and Ozawa (2011).

385 The partial topotaxy observed in kelyphite II is puzzling. It was suggested that Zone
386 C marks the beginning of kelyphite II, where the nucleation of plagioclase took place. It is
387 natural that non-topotaxic relationship between Opx and spinel in kelyphite I is simply
388 inherited to the transition zone and further to the kelyphite II. Observation indicates that
389 spinel gradually gained the topotaxic relationship with its host Opx within the kelyphite II
390 as the kelyphitization advanced. It is puzzling then why spinel gained topotaxic
391 relationship with Opx at such low temperatures, while such relationship is not realized in
392 kelyphite I at earlier stages. The answer to this question may lie in the fact that the degree
393 of supersaturation for reaction (2) may have been smaller than that of reaction (1) because
394 the equilibrium position of the former lies at considerably lower pressures than the latter
395 (Fig. 7). The loss of topotaxic relationship as is seen closer to the garnet, i. e., at later
396 stages, may be ascribed to a further decrease in temperature.

397 Obata and Ozawa (2011) interpreted the presence or absence of topotaxic
398 relationship between Opx and spinel (for kelyphite I) in terms of the degree of
399 supersaturation of the transformation reactions, which may further be related to the
400 transformation temperature (or more accurately, the temperature of nucleation), for the

401 garnet peridotite to spinel peridotite transition. They demonstrated that kelyphite I may be
402 classified into two categories: the high-temperature type, where topotaxy is perfect and the
403 low-temperature type, where topotaxy is imperfect or none. The lack of topotaxial
404 relationship in kelyphite I of the studied sample indicates that this kelyphite belongs to the
405 ‘low-temperature type’ of Obata and Ozawa (2011), which is consistent with the inferred
406 P - T path (Naemura et al, 2009) and the inferred kelyphite-I formation temperature, 730-
407 770°C. Considering all these occurrences and observations, it appears that the boundary
408 between the high- and low-temperature kelyphites lies somewhere between 850°C (for the
409 Czech Mohelno peridotite, Obata and Ozawa, 2011) on one hand and 740-760°C (for the
410 Norwegian peridotite, Obata and Ozawa, 2011) or 730-770°C for the present Czech sample,
411 on the other, and therefore, we tentatively set the boundary temperature at $800\pm 50^\circ\text{C}$
412 (according to the Taylor’s pyroxene geothermometric calibration). It should be noted that
413 this criterion, however, may not apply to kelyphite II, which is a product of a different
414 reaction, as emphasized above.

415 **Origin of the asymmetry of kelyphite II**

416 An important morphological feature of kelyphite II in the Czech sample is that, as
417 emphasized above, it does not form a corona enveloping garnet like ordinary kelyphites in
418 garnet peridotites or eclogites (e.g., Obata, 2011) but it only occurs on one side of garnet.
419 Other isochemical kelyphites reported in the literature (Keankeo et al, 2000; Sapienza et al,
420 2001; Degi et al, 2010), however, occur surrounding relict garnets and so the asymmetric
421 configuration seems to be a unique feature of the Czech sample. The corona structure
422 indicates that the breakdown of garnet occurs from outside of garnet, and more importantly,
423 being initiated by multiple nucleation scattered around the garnet grain surface (see Fig. 20
424 in Obata, 2011). Domain structures typically observed in those kelyphites (Obata and
425 Ozawa, 2011) is considered to be a result of such a multiple nucleation. If nucleation is

426 restricted for some reason or another to one side of the garnet, the symmetry breaks down,
427 resulting in a “unidirectional growth” of symplectite as observed for the spinel-pyroxene
428 symplectite from the Horoman peridotite (Odashima et al, 2008). Odashima et al (2008)
429 argued that the first nucleation would suppress further nucleation because of the high
430 kinetic barrier and high degree of supersaturation of reaction (1). A similar account may be
431 applied to the unidirectional growth of the Czech kelyphite II but, unlike the Horoman
432 sample, kelyphite II is much finer-grained and of lower temperature in origin, and
433 furthermore, the reaction responsible for the formation is different, being reaction (2).
434 Moreover, it is difficult to explain why unidirectional growth occurred only in kelyphite II
435 and not in kelyphite I.

436 We interpret that the unidirectional growth of kelyphite II is the result of
437 suppression of nucleation as advocated by Odashima et al (2008) but consider the reason
438 for the suppression being different. It is noted that the volume increase for reaction (2) is
439 greater than that for reaction (1). (ca. 5% for reaction (1); whereas ca. 15% for reaction (2)
440 relative to garnet; Obata, 2011). So the effect of internal stress is considered to be even
441 greater for the latter than for the former. It is conceivable, therefore, that the initiation of a
442 breakdown of garnet from one side, by reaction (2), will build up a significant internal
443 stress around the garnet, which will suppress further nucleation on other sites. If, however,
444 there were enough time for the built-up stress to relax by deformation of the surroundings,
445 either plastic or brittle deformation, more nucleation may have occurred at other sites, as is
446 the case for kelyphite I (and probably for other isochemical kelyphites in the xenoliths).
447 The observed asymmetric nature of kelyphite II, therefore, implies that the process was so
448 rapid that there was no time allowed for the stress relaxation. This view is consistent with
449 the very fine-grained and dry nature of kelyphite II. The site of the first nucleation may be

450 dictated by some other factors such as fluid infiltration or deformational effects (Odashima,
451 et al, 2008).

452 **Other possible occurrences of isochemical kelyphite**

453 As mentioned in the Introduction, isochemical kelyphite is not uncommon in xenolithic
454 garnet pyroxenites or mafic granulites that lack olivine as a reactant counterpart of garnet
455 (Keankeo et al, 2000; Sapienza et al, 2001; Degi et al, 2010). From orogenic peridotites,
456 one occurrence of “isochemical kelyphite” has been reported in the literature from an
457 orogenic garnet peridotite of Vosges Mts. (France) that also belongs to the Moldanubian
458 zone (Altherr & Kalt, 1996). The lack of detailed description, however, hinders a judgment
459 of whether it really belongs to the same type as we describe here. Although some analyses
460 are said to be “approximately isochemical”, the presence of amphibole in the assemblage
461 and a significant amount of Na in the bulk analysis (1.12%, Table 6; Altherr and Kalt,
462 1996) casts a doubt if it does. Regardless of such uncertainties, we think that there is a good
463 chance that *true* isochemical kelyphites may be found from those rocks. It may be, to some
464 extent, a matter of chance to encounter isochemical kelyphites in randomly-cut rock thin
465 sections and so, we expect to find more isochemical kelyphites from other localities of
466 orogenic peridotite as well as pyroxenite xenolithes. In fact we are finding isochemical
467 kelyphites from a well-studied orogenic peridotite – the Ronda peridotite, Spain (Obata,
468 1980) that has the same features as described above including the asymmetry (work in
469 progress). They are so fine grained that they would be easily overlooked without careful
470 examinations using X-ray compositional mapping and high-resolution electron microscopy.
471 There must also be cases, however, that such isochemical breakdown did not take place at
472 all and that the kelyphitization ceased entirely at the first stage (i.e., formation of kelyphite
473 I). More detailed comparative studies of both cases would be required in order to identify
474 the key factors that control the kelyphitization processes, particularly that of isochemical

475 breakdown of garnet, in terms of P - T paths, cooling and/or ascent rates and availability of
476 fluids in various geotectonic settings.

477 **SUMMARY AND CONCLUDING REMARKS**

478 Isochemical kelyphite (kelyphite II) has been described from a garnet peridotite, Czech
479 Moldanubian Zone. Important observations and conclusions may be summarized as follows.

480 (1) Isochemical kelyphite – kelyphite II – occurs with a transitional zone within ordinary
481 non-isochemical kelyphites – kelyphite I. Furthermore, the kelyphite II is separated from a
482 relict garnet by a thin zone (10-20 μm thickness) of very fine-grained amphibole-spinel
483 symplectite – kelyphite III.

484 (2) An asymmetric configuration of kelyphite II with respect to relict garnets and kelyphite
485 III was emphasized as a unique structural feature for the studied locality.

486 (3) It was concluded that kelyphite I was first formed by the reaction between garnet and
487 olivine. This reaction was apparently ceased leaving some relict garnet in the center of
488 kelyphite I. Upon a further decompression, when the garnet itself became unstable, it got
489 partially broken down forming an isochemical kelyphite – kelyphite II.

490 (4) The transition zone is divided into two subzones: B (Opx+Sp+Amp) and C
491 (Opx+Sp+Pl+Amp). We interpret that subzone B represents an extension of kelyphite I,
492 whereas subzone C is interpreted to mark the onset of the breakdown reaction of garnet,
493 which was followed by the formation of isochemical kelyphite.

494 (5) The asymmetric nature of kelyphite II may be ascribed to a stress build-up due to the
495 volume-increase nature of the kelyphite II-formation reaction that took place rapidly
496 enough not to allow for stress relaxation by deformation.

497 (6) It was hypothesized that the second reaction (i.e., isochemical breakdown of garnet) has
498 been stopped by the third, hydration reaction that formed a thin hydrous zone, kelyphite III,
499 at the reaction front of kelyphite II.

500 (7) The absence of topotaxial relationships between Opx and spinel in kelyphite I implies
501 that the studied Czech sample belongs to the ‘low-temperature type’ kelyphite of Obata and
502 Ozawa (2011); whereas partial topotaxy observed in kelyphite II suggests that the degree of
503 supersaturation of the relevant reaction was not that great, despite of the inferred low
504 temperatures of the transformation.

505 (8) It is not conclusive whether the formation of kelyphite I and that of kelyphite II form a
506 consecutive single process or represents distinct events separated in both time and physical
507 conditions.

508 (9) It is proposed that the boundary between the high- and low-temperature kelyphites (for
509 kelyphite I) lies around $800\pm 50^{\circ}\text{C}$.

510 Isochemical kelyphite may be more widespread in orogenic peridotites than
511 previously thought. More comparative studies of cases in which isochemical kelyphite is
512 formed and other cases in which kelyphitization has terminated at the kelyphite I stage is
513 needed to clarify the factors controlling the kelyphitization processes and its dynamics.

514

515 **ACKNOWLEDGEMENTS**

516 We are grateful to Prof. T. Hirajima (Kyoto Univ.) and Dr. M. Svojtka (Academy of
517 Science, Czech Republic) for their cooperations in the field and for discussions. We are
518 also grateful to Prof. H. Nagahara for her permission of the use of FE-SEM and EBSD
519 facilities at Univ. Tokyo, and to Dr. H. Yoshida for his technical assistance and to Professor
520 Emeritus I. Kushiro for his discussions on the garnet breakdown reactions. Thanks are
521 extended to Dr. T. Kawakami and T. Ueda for their assistance in the microprobe work, to
522 Dr. Seto Y. (Kobe Univ.) for his assistance with the TEM analytical work and to Mr.
523 Tutumi for his thin section preparations. The paper was benefitted by constructive

524 criticisms of Petr Jerabek and an anonymous reviewer and their efforts are acknowledged.

525 Editorial handling by R. Abart is greatly acknowledged.

526

526 **REFERENCES CITED**

- 527 Altherr A, Kalt A (1996) Metamorphic evolution of ultrahigh-pressure garnet peridotites from the
528 Variscan Vosges Mts. (France). *Chemical Geology* 134: 27–47.
- 529 Bailey SW, Frank-Kamenetskii VA, Goldshtaub SA, Kato A, Pabst H, Schlz H, Taylor HFW,
530 Wilson AJC (1977) Report of the International Mineralogical Association (IMA)-International
531 Union of Crystallography (IUCr) Joint Committee on Nomenclature, *Acta Cryst.* A33: 681-684.
- 532 Chopin C (1984) Coesite and pure pyrope in high-grade blueschists of the Western Alps; a first
533 record and some consequences. *Contrib Mineral Petrol* 86: 107-118.
- 534 Degi J, Abart R, Kalman T, Bali E, Wirth R, Rhede D (2010) Symplectite formation during
535 decompression induced garnet breakdown in lower crustal mafic granulite xenoliths:
536 mechanisms and rates. *Contrib. Mineral. Petrol.* 159: 293-314.
- 537 Gasparik T (1984) Two-pyroxene thermobarometry with new experimental data in the system CaO-
538 MgO-Al₂O₃-SiO₂. *Contrib. Mineral Petrol* 87: 87-97.
- 539 Gillet P, Ingen J, Chopin, C (1984) Coesite in subducted continental crust: *P–T* history deduced
540 from an elastic model. *Earth Planet Sci Lett* 70: 426-436.
- 541 Green ECR, Holland TJB, Powell R, White RW (2012) Garnet and spinel lherzolite assemblages in
542 MgO-Al₂O₃-SiO₂ and CaO-MgO-Al₂O₃-SiO₂ : thermodynamic models and an
543 experimental conflict. *J Metamorphic Geol* 30: 561-577.
- 544 Keaneko W, Taylor WR, FitzGerald JD (2000) Clinoferrosilite-bearing kelyphite: a breakdown
545 product of xenolithic garnet, Delegate breccia pipes, New South Wales, Australia. *Mineralogical*
546 *Magazine* 64(3): 469-479.
- 547 Kushiro I, Yoder HS Jr (1966) Anorthite-forsterite and anorthite-enstatite reactions and their
548 bearing on the basalt eclogite transformation. *J Petrol* 7: 337-362.
- 549 Medaris LG, Wang HF, Jelínek E, Jakeš P (2005) Characteristics and origins of diverse Variscan
550 peridotites in the Gföhl Nappe, Bohemian Massif, Czech Republic. *Lithos* 82: 1-23.

- 551 Milke R, Abart R, Kunze K, Koch-Müller M, Schmid D, Ulmer P (2009) Matrix rheology effects
552 on reaction rim growth I: evidence from orthopyroxene rim growth experiments. *J*
553 *Metamorphic Geol* 27: 71-82.
- 554 Naemura K, Hirajima T, Svojtka M (2009) The pressure-temperature path and the origin of
555 phlogopite in spinel–garnet peridotites from the Blansky Les Massif of the Moldanubian Zone,
556 Czech Republic. *J. Petrology* 50: 1795-1827.
- 557 Obata M, Ozawa K (2011) Topotaxial relationships between spinel and pyroxene in kelyphite after
558 garnet in mantle-derived peridotites and their implications to reaction mechanism and kinetics.
559 *Mineralogy and Petrology* 101: 217-224.
- 560 Obata M (2011) Kelyphite and symplectite: textural and mineralogical diversities and universality,
561 and a new dynamic view of their structural formation. in *New Frontiers in Tectonic Research*,
562 Sharkov, E. V. (Ed.), ISBN: 978-953-307-595-2, InTech, pp. 350.
- 563 Odashima N, Morishita T, Ozawa K, Nagahara H, Tsuchiyama A, Nagashima R (2008) Formation
564 and deformation mechanisms of pyroxene-spinel symplectite in an ascending mantle, the
565 Horoman peridotite complex, Japan: An EBSD (electron backscatter diffraction) study. *Jour of*
566 *Mineral and Petrol Sciences* 103: 1-15.
- 567 O'Hara M (1967) Mineral paragenesis in ultrabasic rocks. In Wyllie, P. J. (ed.) *Ultramafic and*
568 *Related Rocks*. New York: John Wiley & Sons, 393-401.
- 569 O'Hara M, Richardson SW, Wilson G (1971) Garnet peridotite stability and occurrence in crust and
570 mantle. *Contrib Mineral Petrol* 32: 48-68.
- 571 Sapienza G, Scribano V, Calvari S (2001) Kelyphitic breakdown of garnets from pyroxenite
572 xenoliths, south-eastern Sicily, Italy. *Periodico de Mineralogia* 70 (3): 377-386.
- 573 Schmid DW, Abart R, Podladchikov YY, Milke R (2009) Matrix rheology effects on reaction rim
574 growth II: coupled diffusion and creep model. *J Metamorphic Geol* 27: 83-91.
- 575 Stipska P, Powell R (2005) Constraining the P – T path of a MORB-type eclogite using
576 pseudosections, garnet zoning and garnet-clinopyroxene thermometry: an example from the
577 Bohemian Massif. *J Metamorphic Geol* 23: 725-743.

578 Taylor WR (1998) An experimental test of some geothermometer and barometer formulation for
579 upper mantle peridotites with application to the thermobarometry of fertile lherzolite and garnet
580 websterite. Neues Jahrbuch fur Mineralogie Abhandlungen 172: 381-408.

581

582

582 **FIGURE CAPTIONS**

583 Figure 1. (a) Geotectonic subdivision of the Variscan orogen in central Europe and (b)
584 simplified geologic map of the studied area showing the sample locality. P, Prahatic
585 massif; K, Kristanov massif; BL, Blansky les massif; L, Lisov massif. The studied
586 peridotite is from the Plešovice quarry (indicated by a star) within Blansky les massif.
587 Modified from Naemura et al. (2009).

588 Figure 2a. Optical photomicrograph (plane polarized light) of a garnet peridotite, sample
589 PL4, that contains three kinds of kelyphites, I, II and III (abbreviated as Kely I, II and
590 III, respectively). Frame (α) is the area of Fig. 3 and that of (β) is for Fig. 4a.

591 Figure 2b. Optical photomicrograph with crossed polarized light and a gypsum plate to
592 emphasize the domain structure of kelyphites, which is recognized with the lineament
593 structure and the interference color. Central part of the area of Fig. 2a. Points (b), (c)
594 and (d) in kelyphite II indicate positions where crystallographic orientation data
595 plotted in Fig. 5 (b, c, d) were obtained.

596 Figure 3. X-ray compositional maps (Al, Ca, Mg, Fe) of the kelyphites and their
597 surroundings. Area (α) in Fig. 2a. Warmer colors represent higher contents of
598 respective elements. Kelyphite II is nearly isochemical with garnet except along
599 fracture veins ("f" in Fig. 4a), where slight depletion in Ca and enrichment in Mg and
600 Na (not shown here) are noted. Note that kelyphite III is not isochemical.

601 Figure 4. (a) Back scattered electron images (BSE) of the kelyphites and their
602 surroundings (area β in Fig. 2a). Abbreviations are the same as in Fig. 2. 'Trans' is a
603 transition zone between kelyphites I and II; 'f', fracture veins that are either void or
604 filled with unidentified hydrous minerals. Frames (b), (c), (d) and (e) indicate the
605 areas of the following photographs: (b) Kelyphites I, II and III. Domains in kelyphite
606 II are labeled 1, 2 and 3 and the domain boundaries and transition zone are indicated

607 by white lines. Black areas are either voids or unidentified hydrous phases of
608 probable secondary origin. (c) coarse grained Opx and spinel in kelyphite II as
609 indicated by an arrow; (d) A close up of the transition zone, between kelyphite I
610 (Opx+Cpx+Sp±Amp: Zone A) and kelyphite II (Opx+Sp+Pl: Zone D). The transition
611 zone may be subdivided into two subzones, B (Opx+Sp+Amp) and C (Opx+Sp+Pl+
612 Amp). The domain boundary in kelyphite II is indicated by white dashed lines. The
613 domains are labeled 1, 2, 3 as in (b). Frame (c) is the area of photograph 4(c). The
614 area where gentle curvatures occur in the lineament is indicated with a white dotted
615 circle near the outer margin of kelyphite II (domain 3) (see text for more details). (e)
616 Transition subzones B and C, and kelyphites I, II and III around garnet. In the upper
617 half of the photograph, a transition subzone B is directly juxtaposed to kelyphite II
618 (Zone D) without subzone C, where internal structure of Zone B is sharply truncated
619 by kelyphite II. In the lower-half, the same zone B is directly juxtaposed to the
620 garnet, without Zone C in between. Note a narrow zone of kelyphite III developed
621 between kelyphite II and garnet. Kelyphite III is a vermicular intergrowth of
622 amphibole (gray), thin numerous spinel lamellae (lighter colored) and subordinate
623 amount of plagioclase (the darkest) nearly perpendicular to the garnet surface. 'f' is
624 fracture vein (See (a) for explanation). A white circle marked 's' in an Opx–spinel
625 symplectite in Zone B indicates the area where bulk chemical analysis (Table 2, No.
626 11) was obtained.

627 Figure 5. Pole figure plots of Opx and spinel from domain 3 of kelyphite II. (a) Opx; (b)
628 spinels from outer margin of the domain; (c) spinels from the central part of the
629 domain; (d) spinels from deep inner part close to kelyphite III. Approximate areas
630 where these data were obtained are indicated as (b), (c) and (d), respectively, in Fig.

631 2b. Small circles in (c) represent approximate areas of Opx (100) and (010),
632 respectively, defined by the Opx data in (a).

633 Figure 6. Pole figure plots for amphibole (a) and spinel (b) from kelyphite III adjacent to
634 kelyphite II domain 3. Note that the orientation of amphibole is nearly coincidental
635 with that of Opx in the adjacent kelyphite II (Fig. 5(a)).

636 Figure 7. Inferred relative timing of the formation of kelyphites I and II marked on a P - T
637 path for the Plešovice peridotite (modified from Naemura et al. 2009). Reaction
638 boundaries (1) for $Ol+Grt = Opx+Cpx+Sp$; (3) for $Grt = Opx+Cpx+Sp+An$; and (5)
639 for $Ol+An = Opx+Cpx+Sp$, are theoretical calculations for the system $CaO-MgO-$
640 $Al_2O_3-SiO_2$, compiled by Gasparik (1984) and Green et al, (2012). Boundary (1') is
641 that for the garnet lherzolite to spinel lherzolite transition experimentally determined
642 for a Cr-bearing natural lherzolite, after O'Hara et al, (1971). Kelyphite I formed at
643 Point 1 in the ariegite-facies field. Two possibilities are indicated for the kelyphite II
644 formation: Point 2 at slightly higher pressure than equilibrium position (3) (thus in the
645 ariegite-facies field but below Point 1) or; Point 2', which is plotted at lower
646 pressures than reaction (3) in the seiland-facies field (see text for more details). GL ,
647 garnet-lherzolite facies; Ar , ariegite subfacies of spinel-lherzolite facies; Se , seiland
648 subfacies of spinel-lherzolite facies; PL , plagioclase-lherzolite facies (O'Hara, 1967).

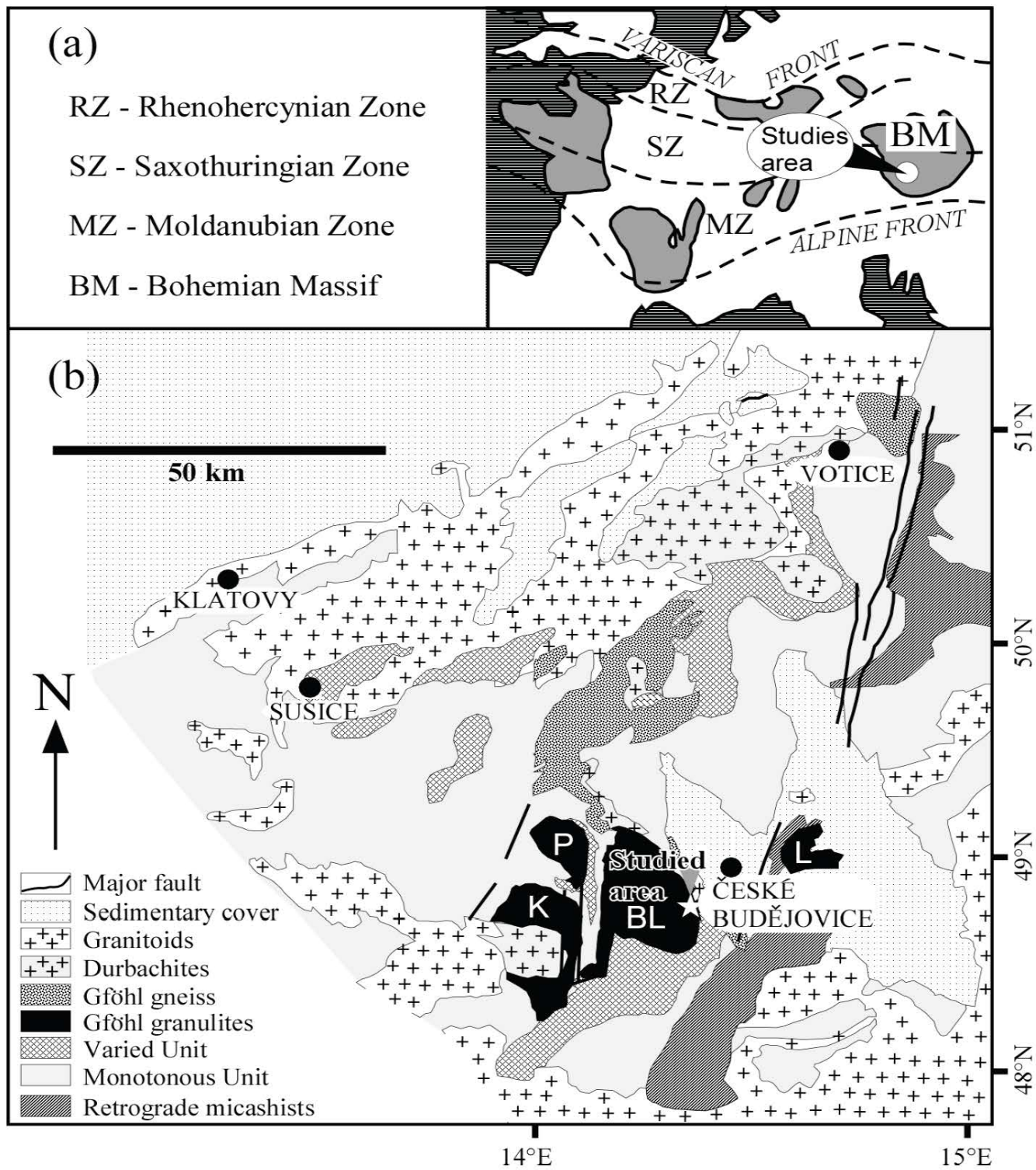


Fig. 1 Obata

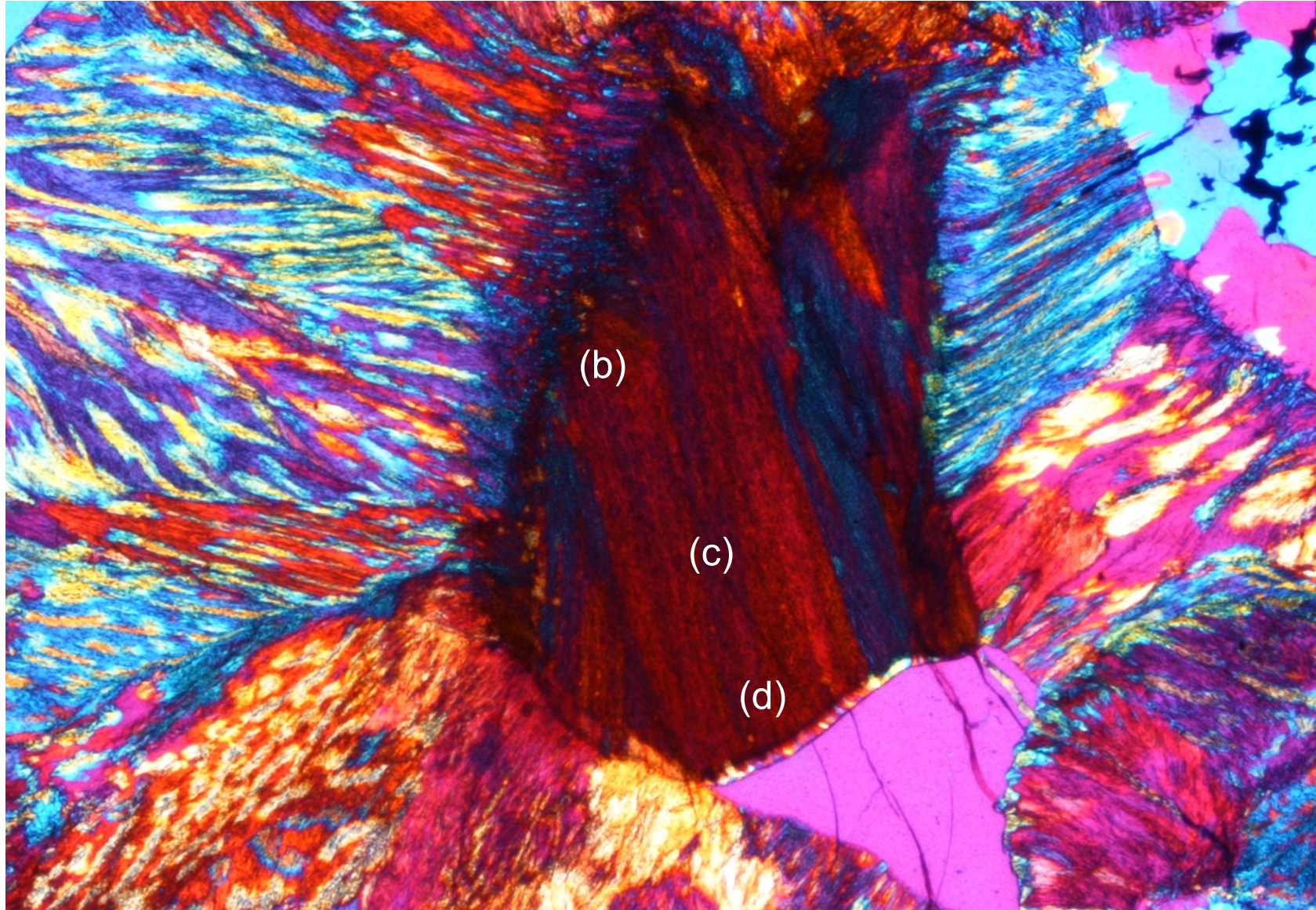


Fig 2b Obata

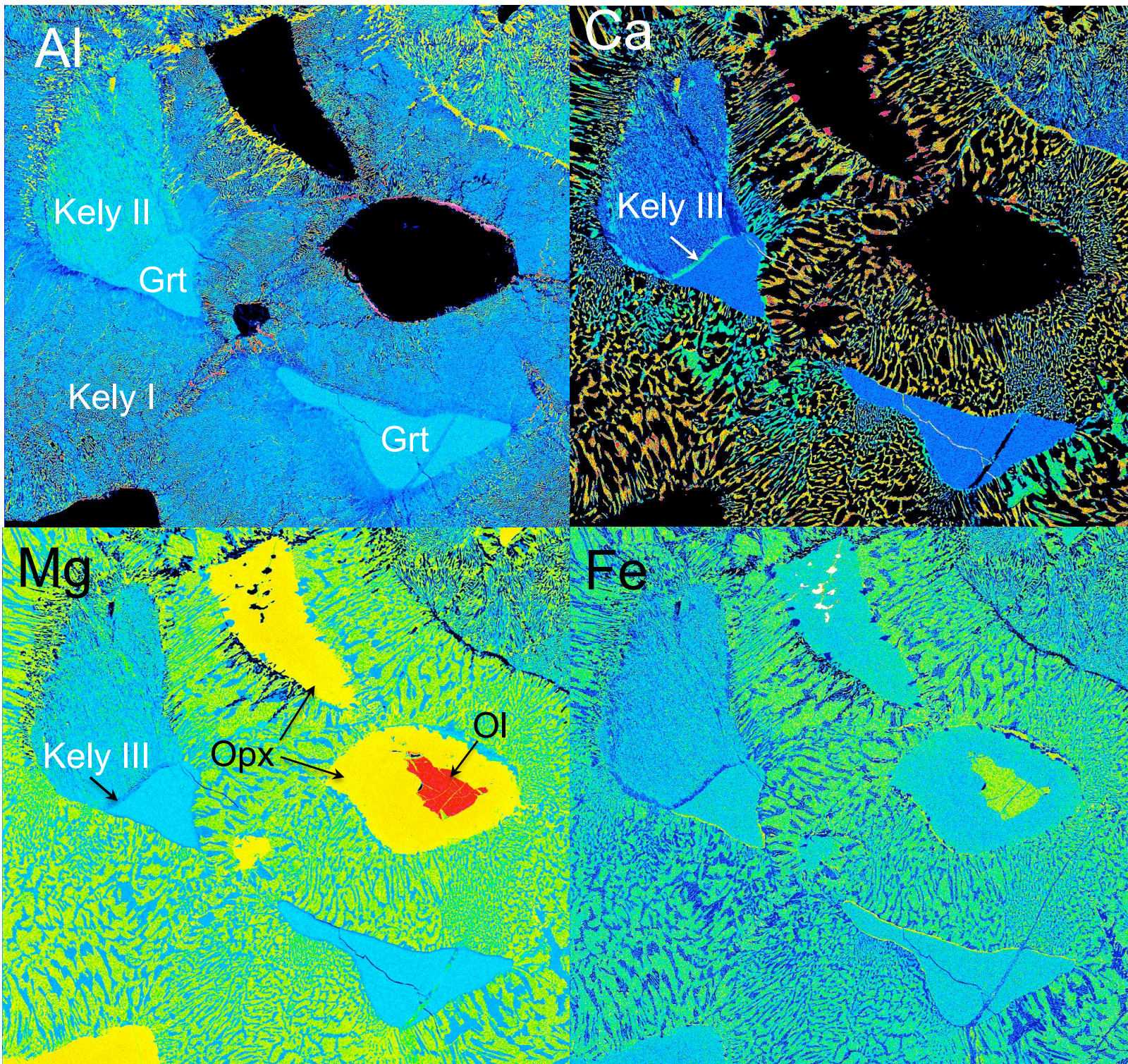


Fig. 3. Obata

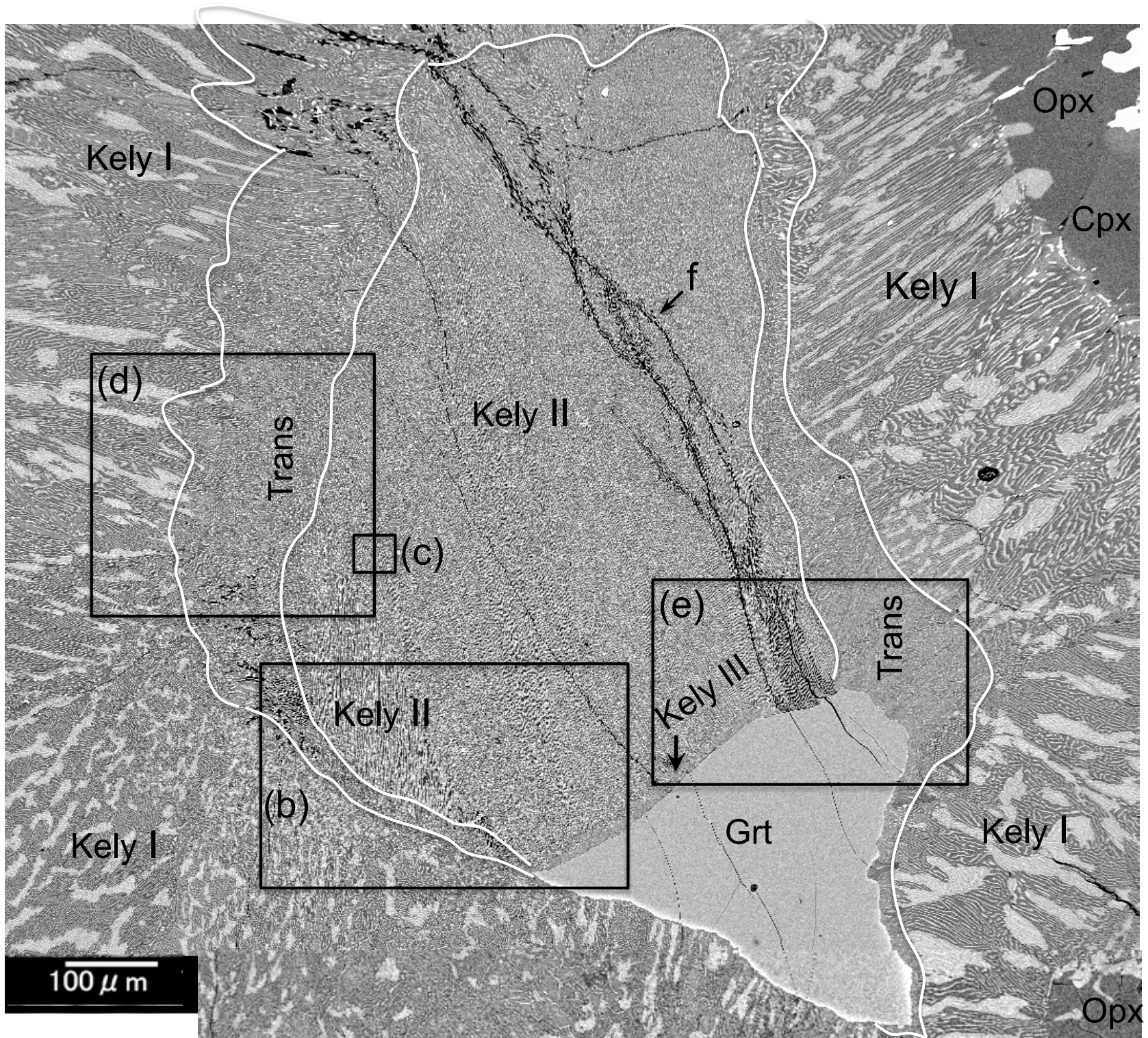


Fig. 4a Obata

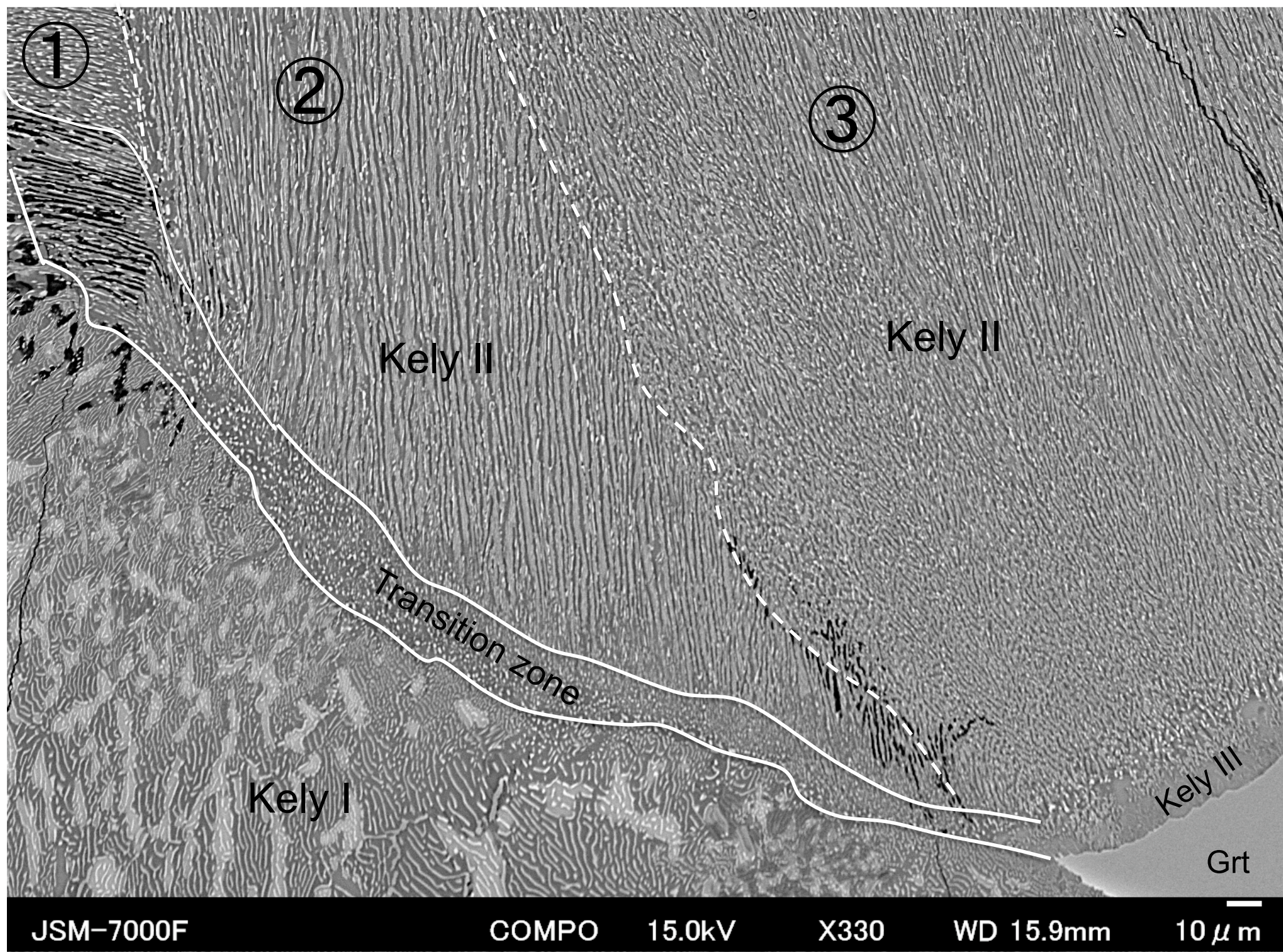


Fig. 4b Obata

JSM-7000F

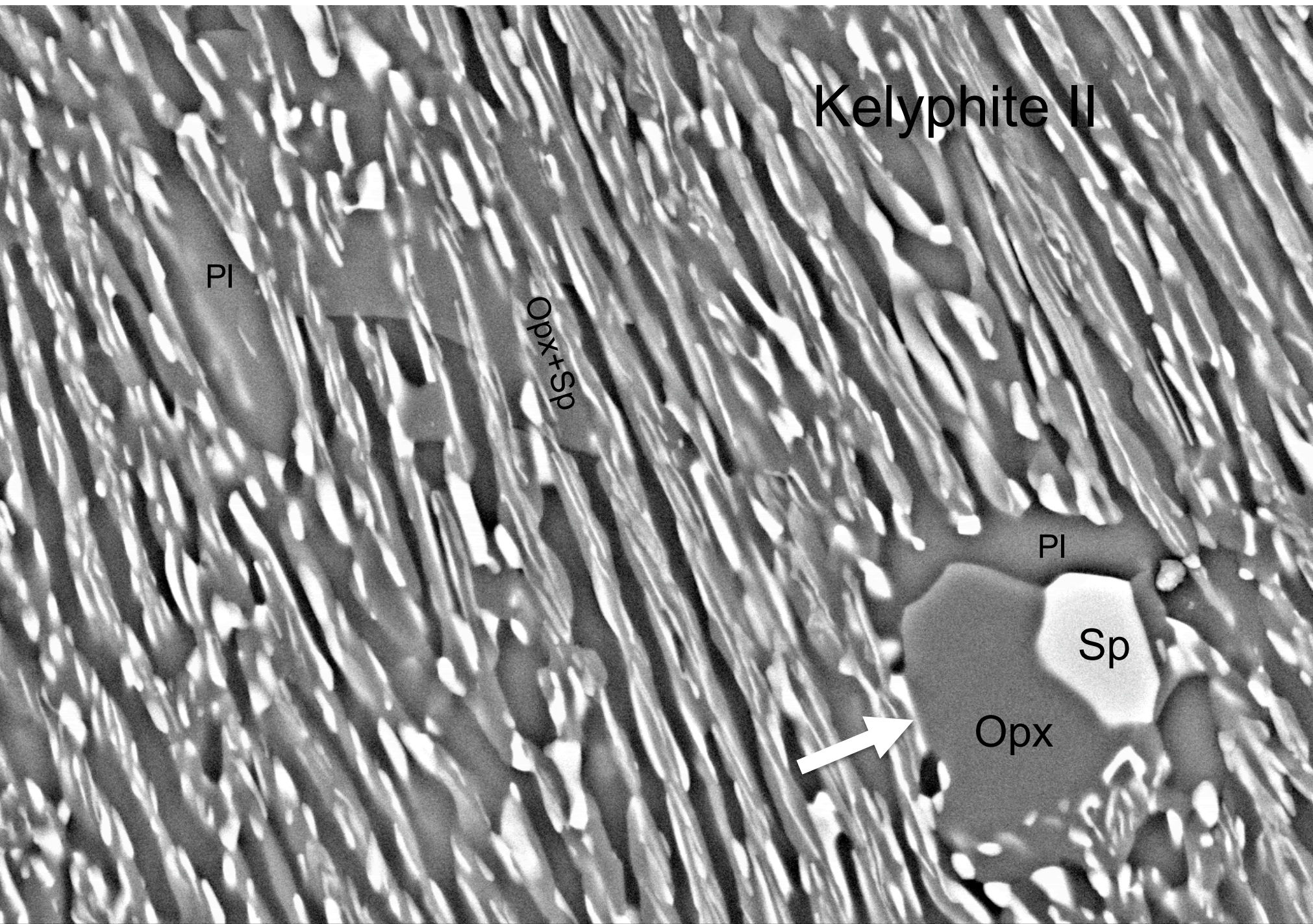
COMPO

15.0kV

X330

WD 15.9mm

10 μm



Kelyphite II

Pl

Opx+Sp

Pl

Sp

Opx



Fig. 4c Obata

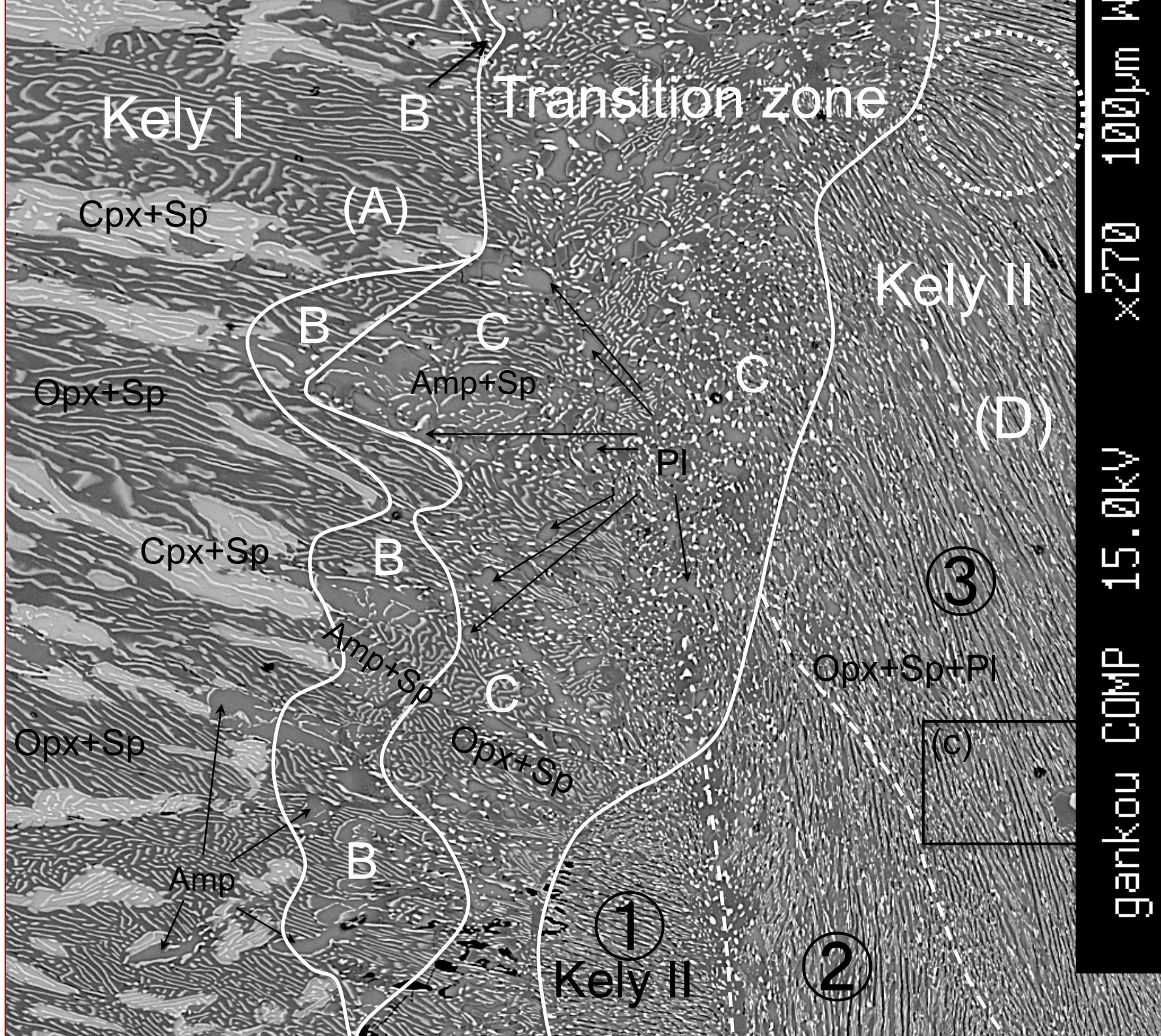


Fig. 4d Obata

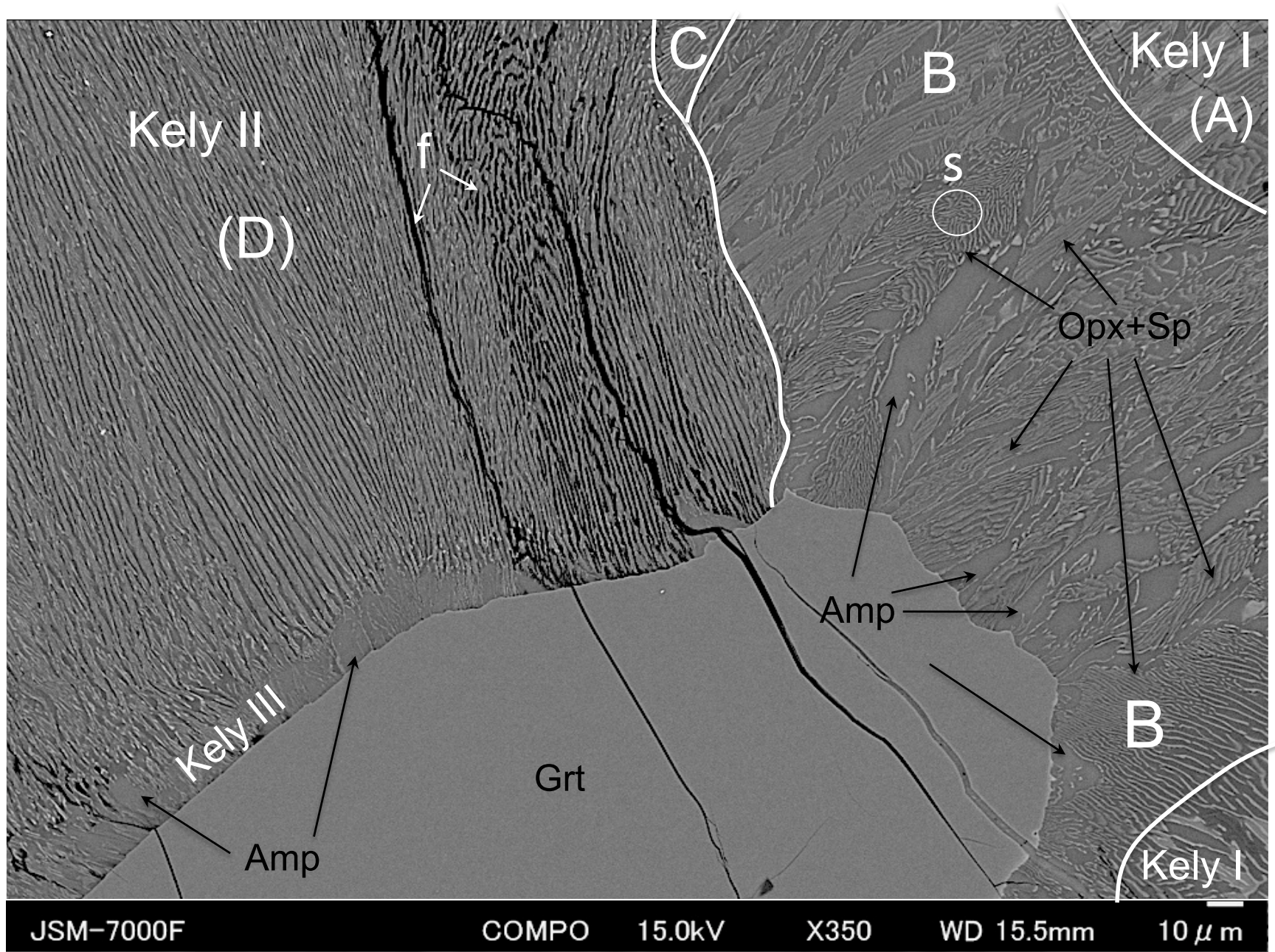


Fig. 4e Obata

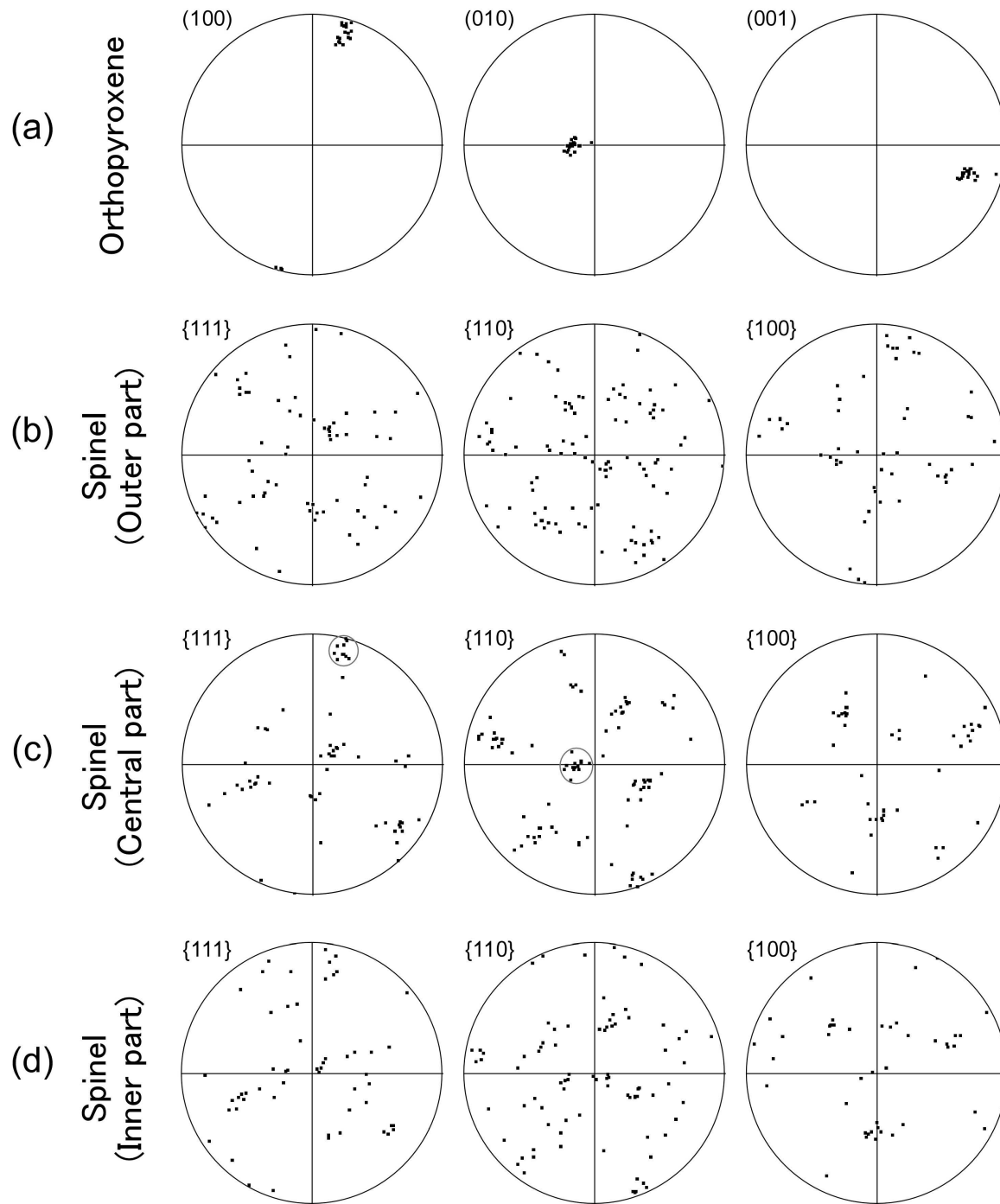


Fig. 5 Obata

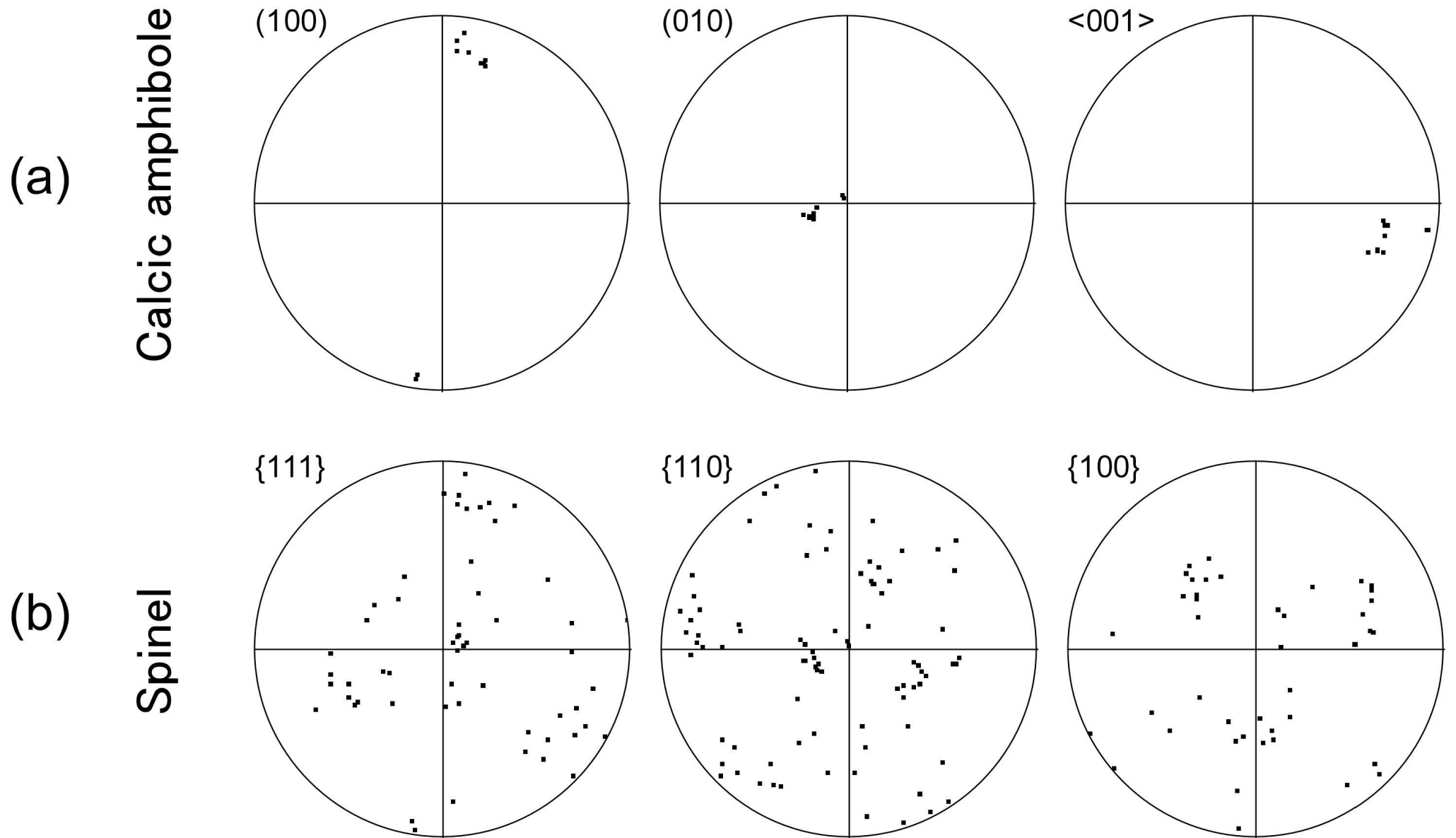


Fig. 6 Obata

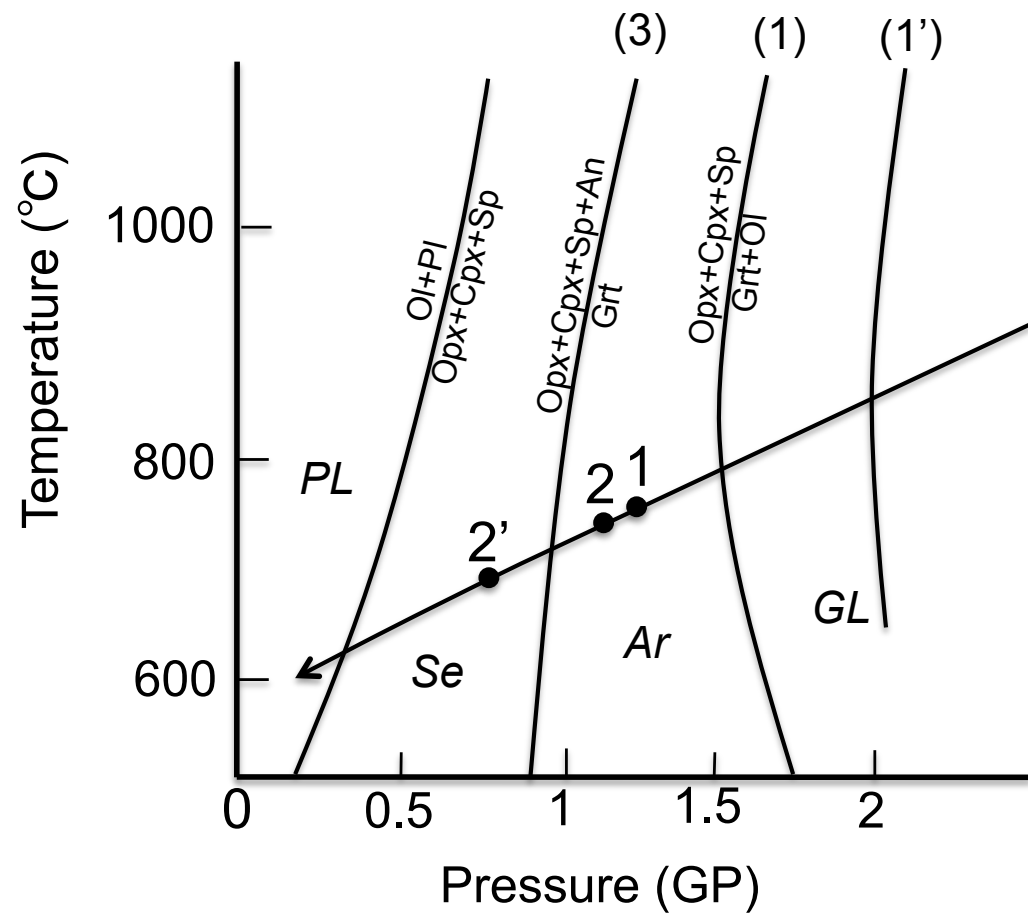


Fig. 7 Obata

TABLE 1. MICROPROBE ANALYSES OF GARNET AND BULK COMPOSITIONS
OF THREE KINDS OF KELYPHITES

	Grt		Kely I		Kely II		Kely III	
	(13)	σ	(22)	σ	(43)	σ	(8)	σ
SiO ₂	42.60	0.31	43.61	1.61	42.95	0.51	41.69	1.00
TiO ₂	0.08	0.08	0.08	0.07	0.05	0.07	0.14	0.15
Al ₂ O ₃	21.94	0.16	16.48	2.14	22.31	1.21	19.86	1.73
Cr ₂ O ₃	3.07	0.08	3.01	0.18	3.08	0.12	2.84	0.11
FeO*	7.46	0.84	6.86	0.57	6.48	0.40	3.56	0.46
MnO	0.34	0.06	0.24	0.03	0.25	0.04	0.14	0.04
MgO	20.20	0.63	26.33	2.05	20.09	1.41	16.69	2.16
CaO	6.04	0.13	6.09	2.72	6.41	0.82	11.33	1.38
Na ₂ O	0.01	0.01	0.04	0.03	0.04	0.02	1.38	0.19
K ₂ O	0.00	0.01	0.00	0.01	0.01	0.01	0.01	0.01
TOTAL	101.73		102.75		101.67		97.65	
O	12		12		12		23	
Si	2.99	0.01	3.05	0.11	3.00	0.03	5.86	0.15
Ti	0.00	0.00	0.00	0.00	0.00	0.00	0.01	0.02
Al	1.82	0.01	1.36	0.18	1.84	0.10	3.29	0.28
Cr	0.17	0.00	0.17	0.01	0.17	0.01	0.32	0.01
Fe ²⁺	0.44	0.05	0.40	0.03	0.38	0.02	0.42	0.05
Mn	0.02	0.00	0.01	0.00	0.01	0.00	0.02	0.00
Mg	2.11	0.06	2.74	0.20	2.09	0.14	3.50	0.45
Ca	0.45	0.01	0.46	0.21	0.48	0.06	1.71	0.21
Na	0.00	0.00	0.01	0.00	0.01	0.00	0.38	0.05
K	0.00	0.00	0.00	0.00	0.00	0.00	0.00	0.00
Sum	8.01		8.19		7.99		15.51	
Mg#	82.8		87.3		84.7		89.3	

Grt, garnet; Kely I, II, III are kelyphites I, II, III, respectively. FeO* as total iron.
 σ , one sigma calculated from numbers of microprobe analyses.
 numbers in () are those of analyses used to obtain each average.

TABLE 2. MICROPROBE ANALYSES OF MINERALS

No.	1	2	3	4	5	6	7	8	9	10	11
Phase:	Grt	Grt	Opx	Opx	Ol	Sp	Plag	Amp	Amp	Amp	Opx+Sp
SiO ₂	42.60	41.58	56.19	55.75	41.46	0.75	43.43	45.97	43.60	43.22	39.99
TiO ₂	0.08	0.09	0.08	0.05	0.02	0.01	0.05	0.59	0.16	0.41	0.02
Al ₂ O ₃	21.94	21.20	3.67	4.00	0.00	57.47	36.08	13.33	17.47	17.46	21.12
Cr ₂ O ₃	3.07	2.99	0.34	0.39	0.01	12.22	0.23	1.25	2.20	2.88	2.88
FeO*	7.46	11.85	7.88	6.80	10.07	11.68	0.40	2.88	3.13	3.17	8.22
MnO	0.34	1.30	0.40	0.36	0.23	0.22	n.d.	0.08	0.13	0.10	0.32
MgO	20.20	16.04	33.11	33.06	49.40	19.26	0.38	18.49	16.57	16.07	28.51
CaO	6.04	5.79	0.29	0.23	0.02	0.11	19.42	12.68	12.18	12.00	0.13
Na ₂ O	0.01	0.01	0.01	0.01	n.d.	n.d.	0.12	1.62	2.23	1.71	0.01
K ₂ O	n.d.	n.d.	n.d.	0.01	n.d.	n.d.	0.01	n.d.	n.d.	0.03	0.01
TOTAL	101.73	100.84	101.97	100.64	101.21	101.73	100.13	96.90	97.68	97.04	101.22
Texture remark		rim	Kely I	large grain in Kely II	adjacen t to COR	large grain in Kely II	zone C	zone B	zone B	Kely III	Opx-Sp symplec. Zone B
O	12	12	6	6	4	12	8	23	23	6.11	
Si	2.99	3.02	1.92	1.92	1.00	0.06	2.01	6.48	6.13	0.04	
Ti	0.00	0.00	0.00	0.00	0.00	0.00	0.00	0.06	0.02	2.91	
Al	1.82	1.81	0.15	0.16	0.00	5.20	1.97	2.22	2.89	0.32	
Cr	0.17	0.17	0.01	0.01	0.00	0.74	0.01	0.14	0.24	0.38	
Fe ²⁺	0.44	0.72	0.22	0.20	0.20	0.75	0.02	0.34	0.37	0.01	
Mn	0.02	0.08	0.01	0.01	0.00	0.01	0.00	0.01	0.02	3.39	
Mg	2.11	1.73	1.68	1.69	1.78	2.20	0.03	3.89	3.47	0.00	
Ca	0.45	0.45	0.01	0.01	0.00	0.01	0.96	1.92	1.84	1.82	
Na	0.00	0.00	0.00	0.00	0.00	0.00	0.01	0.44	0.61	0.47	
Sum	8.01	7.99	4.00	4.00	3.00	8.97	5.01	15.50	15.59	0.00	
Mg#	82.8	70.7	88.2	89.7	89.7	74.6	62.8	92.0	90.4	90.0	

n.d. means under the detection limit. 1, relict garnet, 2, garnet rim facing kelyphite I; 3, Opx in kelyphite I;

4, Opx in kelyphite II; 5, primary olivine adjacent to COR-Opx; 6, spinel in kelyphite II;

7, plagioclase in the transition sub-zone C; 8 and 9, amphibole in the transition sub-zone B; 10, amphibole in kelyphite III; 11, bulk analysis of Opx-Sp symplectite in transition sub-zone B, obtained using defocused electron beam (5 μm diameter) (see circle in Fig. 4e).